

General Disclaimer

One or more of the Following Statements may affect this Document

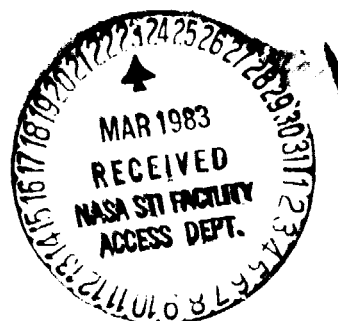
- This document has been reproduced from the best copy furnished by the organizational source. It is being released in the interest of making available as much information as possible.
- This document may contain data, which exceeds the sheet parameters. It was furnished in this condition by the organizational source and is the best copy available.
- This document may contain tone-on-tone or color graphs, charts and/or pictures, which have been reproduced in black and white.
- This document is paginated as submitted by the original source.
- Portions of this document are not fully legible due to the historical nature of some of the material. However, it is the best reproduction available from the original submission.

Summary Report

FEASIBILITY ANALYSES OF ELECTROEPITAXIAL R&D ACCOMMODATIONS

Volume II - Electroepitaxial Growth of GaAs

April 1982



(NASA-CR-170728) FEASIBILITY ANALYSES OF
ELECTROEPITAXIAL RESEARCH AND DEVELOPMENT
ACCOMMODATIONS. VOLUME 2: ELECTROEPITAXIAL
GROWTH OF GaAs Summary Report (Teledyne
Brown Engineering) 23 p HC A02/MF A01

N83-20791

Unclas
G3/76 03047

 **TELEDYNE
BROWN ENGINEERING**

Cummings Research Park • Huntsville, Alabama 35801

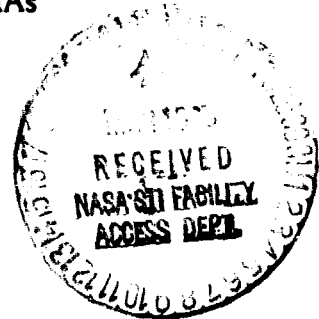
**SUMMARY REPORT
SP82-MSFC-2591**

**FEASIBILITY ANALYSES OF ELECTROEPITAXIAL
R&D ACCOMMODATIONS**

VOLUME II

ELECTROEPITAXIAL GROWTH OF GaAs

APRIL 1982



PREPARED FOR

**GEORGE C. MARSHALL SPACE FLIGHT CENTER
MARSHALL SPACE FLIGHT CENTER, ALABAMA 35812**

CONTRACT NO. NAS8-34743

PREPARED BY

**SPACE SYSTEMS DEPARTMENT
TELEDYNE BROWN ENGINEERING
HUNTSVILLE, ALABAMA**

FOREWORD

A study to determine the feasibility of accommodating the R&D requirements of electroepitaxial crystal growth in the Space Shuttle has been performed. The specific accommodations facilities studied were the Orbiter Middeck stowage lockers, Materials Experiment Assembly (MEA), and Get Away Special (GAS) Cans. The effort has encompassed development of guidelines and assumptions necessary to quantify and characterize elements of the electroepitaxial process, conceptual design of a Gallium Arsenide Crystal Growth Facility, and assessment of facility requirements versus Orbiter Middeck, MEA, and GAS Can capability.

The results of this study indicates that the MEA can best accommodate the R&D furnace facility. The Middeck area, though marginally suitable, has energy, heat rejection, volume, and safety concerns. The GAS Can program ground rules prohibit its use for this application.

This study was performed by Teledyne Brown Engineering under Contract NAS8-34743.

APPROVED:



C. E. Kaylor
Project Manager

TABLE OF CONTENTS

	Page
INTRODUCTION	1
PROCESS PHYSICS	1
PRESENT LABORATORY TECHNIQUE	7
EXPERIMENTAL RESULTS IMPORTANT TO SPACE PROCESSING	7
GRAVITY RELATED CRYSTAL GROWTH DYNAMICS	10
REFERENCES	18

LIST OF FIGURES

Figure	Title	Page
1	Temperature Composition Phase Diagram For GaAs	4
2	Equilibrium Partial Pressures of the GaAs System	5
3	Deposition Rate Vs. Arrival Rate of As ₂	6
4	Laboratory Facility	8
5	Effect of Current Density on Growth Rate	9
6	Effect of Temperature on Growth Rate	11
7	Horizontal Temperature Profile in Growth Cell	12
8	Temperature Gradient Across Solution Vs. Electric Power at 902°C	13
9	Effect of Solution Depth on Growth Rate	14
10	Stability Diagram for Convective Flow	16

ELECTROEPITAXIAL GROWTH OF GaAs

Introduction:

Crystal growth processes are phase transformations which are driven by differences in chemical potential between the nutrient and crystallizing phases. An important step in crystal growth is the transport of material from the bulk of the fluid to the growing crystal surface. In the case of melt growth this is achieved by temperature gradient which then dissipates the latent heat of fusion generated by the solidification process. Such temperature gradients in turn generate thermal convection in the melt. Both natural and forced convective flows provide very important sources of enhancing mass transfer required for the growth of a crystal.

One of the techniques used to achieve forced convection is to apply an electric field. This field may change the chemical potential of a species by either polarizing it and/or exerting a force on it equal to the product of the ionic charge of the species and the local electric field strength.

The technique of electromigration, i.e., electric field induced forced convection, can be used to grow semiconductor material and other compounds from solution by passing electric current through the growth interface while the temperature of the system is maintained constant. Current-controlled electromigration, referred to as electroepitaxy, has been successfully applied to grow epitaxial layers of various semiconductors and garnets.

Process Physics:

An electric field can change the chemical potential of a component i by either polarizing it and/or exerting a force on it proportional to the ionic charge of i thereby causing a differential migration, i.e., diffusion. If ionized species are involved, electromigration due to field-charge interaction will typically dominate over the polarization term. The mass transfer under such conditions for the cations and anions are respectively.

$$m_c = +\beta_+ c_+ FE$$

$$m_a = -\beta_- c_- FE$$

Here, β is equivalent conductance, F is the Faraday, and E is the electric field vector. Thus the cations move in the direction of the electric field vector. In general, ions move at different rates and the condition of electroneutrality must be

satisfied. This has several important consequences. Application of an electric field to an initially homogeneous solution causes partial separation of the ions. On the other hand, diffusion in a concentration gradient generates an electric field. Diffusion of one ion into a homogeneous mixture of others can also cause their preferential migration. Crystallization in electrolytes causes electric fields to develop because of different ionic diffusion rates, different tendencies towards incorporation of the different ions by the growing crystals, and differences in the absorption of anions and cations on the crystal surface.

Mixtures of liquid metals are also found to exhibit electromigration. Here, however, the mechanism of relative movement is not as clear as it is for aqueous solutions. One can imagine the metal "ions" to be influenced by the field even though they are immersed in a cloud of electrons. However, recent work suggests that electromigration in liquid alloys is predominantly governed by a momentum exchange arising from nonelastic scattering of the electrons by the ions (1-3).

From the experimental data it can be inferred that the electric current, rather than electric field, is responsible for electromigration in metals. Hence, the mass transfer flux equation should contain electric current terms as the driving force rather than electric field. Experimentally, it has proven difficult to separate the effects of electromigration from the increased stirring generated by the Joule heating and magnetohydrodynamic forces caused by the high current densities (4).

The growth rate during current-controlled electroepitaxy of GaAs can be explained on the basis of Verhoeven's Theory (5) for electromigration in metallic melt solutions. According to Verhoeven, the use of the differential mobility (μ_d) is only rigorously correct in dilute solutions. For more general case, the velocity of the solute is the resultant of the velocities due to diffusion, electromigration, and bulk movement of the interface. Under this condition the flux of the solute towards the interface is given by

$$\phi = -c_a R - \rho_M \bar{V}_b \bar{D} \frac{dc_a}{dz} + c_a c_b \bar{V}_b \mu_d^2 E$$

where c_a and c_b are the concentrations of the two components of the alloy, R is the rate of solidification, \bar{D} is the mutual diffusion coefficient, ρ_M is the molar density, \bar{V}_b is the partial molar volume of the solvent component of the alloy, and E is the electric-field intensity. As an approximation, if the coefficients of c_a are assumed constant, then the effective distribution coefficient can be calculated.

$$k_e = \frac{k_o \left(1 + \frac{c_b \bar{V}_b \mu_d^2 E}{R} \right)}{k_o + \left[1 + \frac{c_b \bar{V}_b \mu_d^2 E}{R} - k_o \right] \exp - \left[\left(1 + \frac{c_b \bar{V}_b \mu_d^2 E}{R} \right) \frac{R \delta}{\rho_M \bar{V}_b \bar{D}} \right]}$$

If the movement of the growth interface and the contribution due to diffusion can be neglected for GaAs electroepitaxy, then the As flux towards the interface can be approximated by

$$\phi_{As} = c_{As} c_{Ga} \bar{V}_{Ga} \mu_d^2 E$$

From a thermodynamic point of view, the key to the GaAs electroepitaxy is that the passage of electric current disturbs the equilibrium concentration of the gallium-arsenic solution by inducing the deposition of GaAs on to the GaAs substrate. Since the solution is saturated with arsenic at the equilibrium operating temperature, the removal of GaAs in the stoichiometric ratio will leave the solution arsenic deficient. To counterbalance, arsenic must be added to the solution. This is achieved through the desolution of a GaAs source material.

The thermodynamic picture for the system is based on the binary phase diagram as depicted in Figure 1. The major, rather unique feature of the phase diagram is that a single liquidus curve covers nearly the entire composition range. The solid and liquid phases of the phase diagram down to quite low temperatures clarify the need and usefulness of the epitaxial growth technique. Moreover, the vapor phase plays a significant role in determining the optimum growth technique. For GaAs at its melting point, the arsenic pressure is of the order of 10 atm. On the Ga-rich portion of the liquidus at around 900 °C, the As pressure is $< 10^{-4}$ atm as shown in Figure 2. This means that electroepitaxy can be carried out in a 1-atm apparatus.

Stoichiometric GaAs is formed as long as the rate of collision between absorbed gallium and impinging arsenic is equal to the arrival rate of gallium. Figure 3 shows schematically the deposition rate as a function of the ratio of arsenic and gallium arrival rates, for a fixed gallium arrival rate. Below $R_{As}/R_{Ga} = 0.5$, the growth is rich in gallium. Stoichiometric growth occurs at and beyond this ratio with a constant deposition rate until, in principle, arsenic begins to condense.

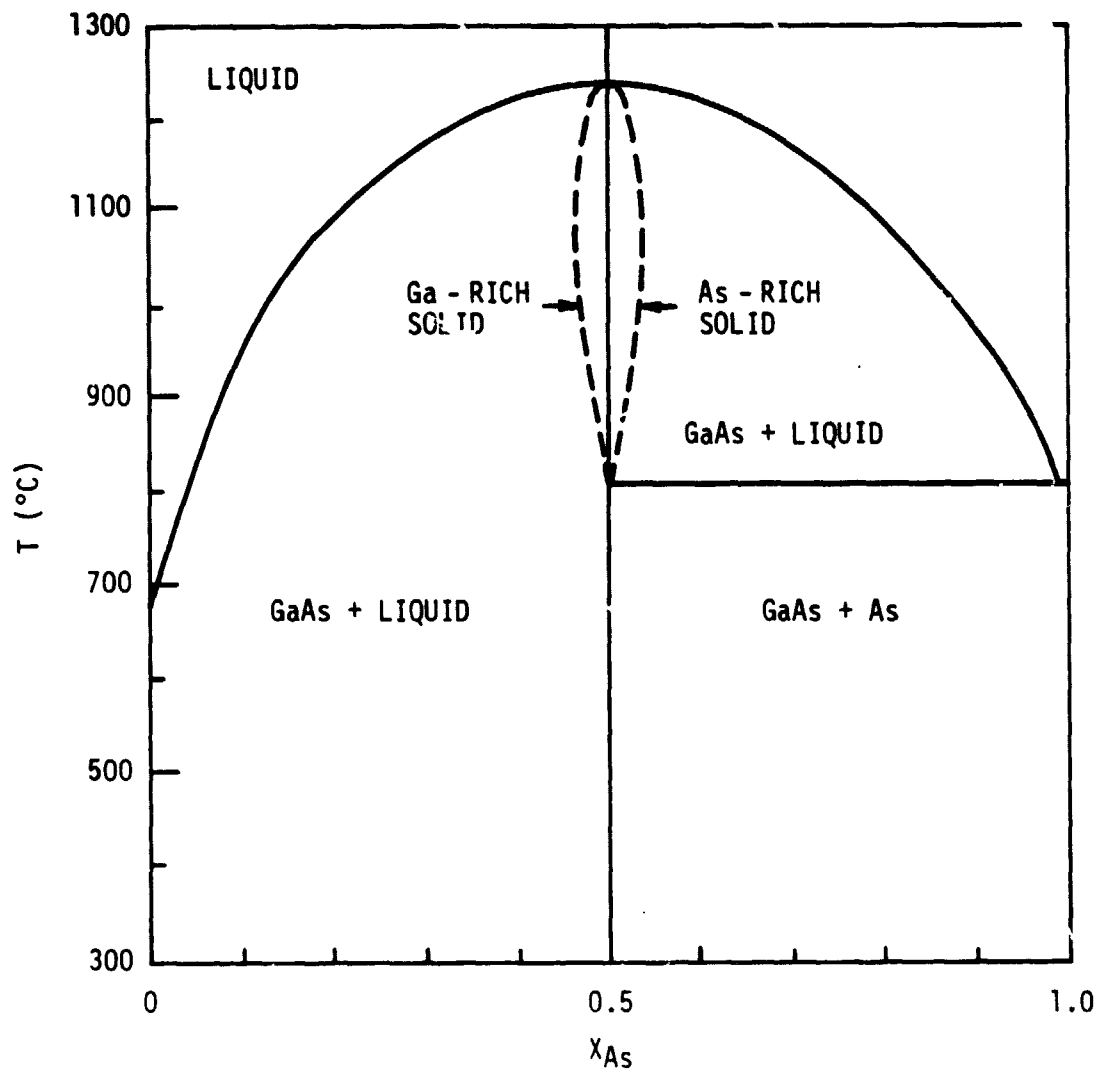


FIGURE 1. TEMPERATURE COMPOSITION PHASE DIAGRAM FOR GaAs

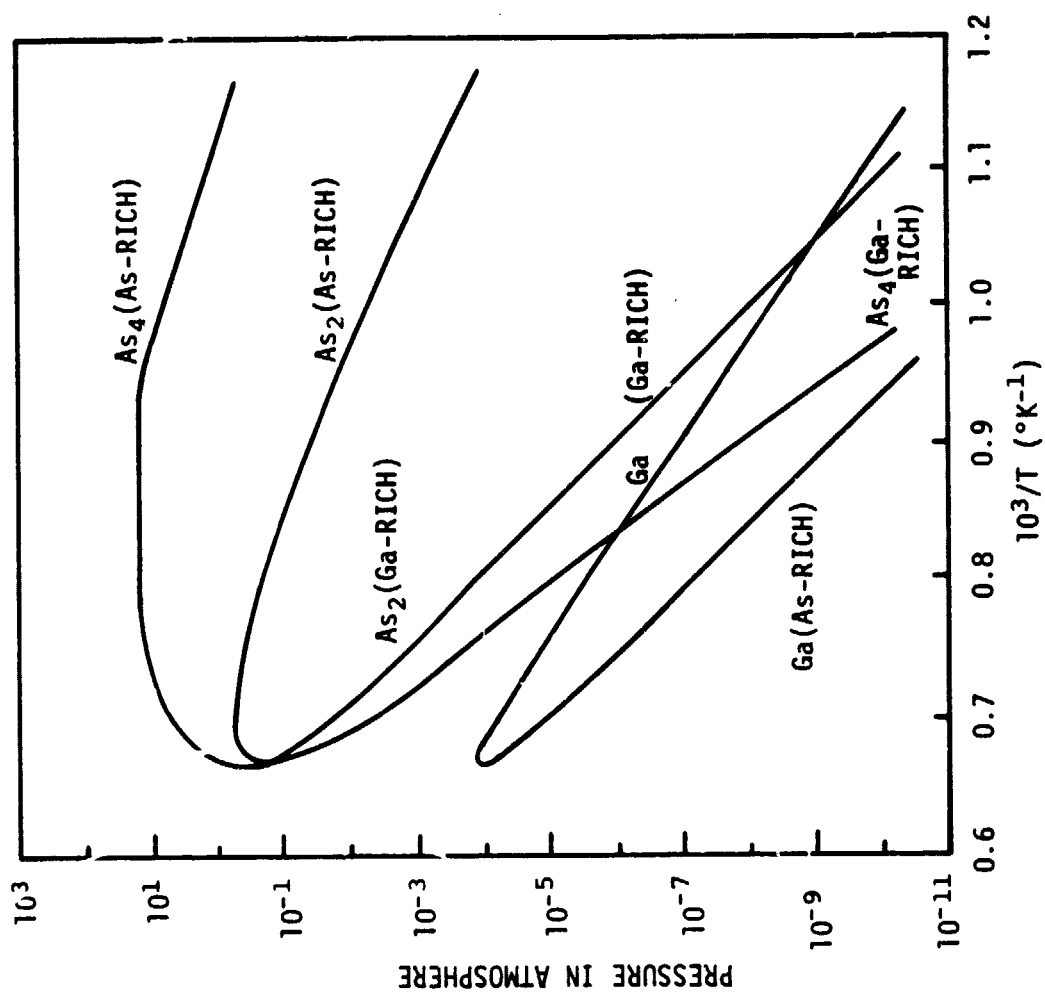


FIGURE 2. EQUILIBRIUM PARTIAL PRESSURES OF THE Ga-As SYSTEM

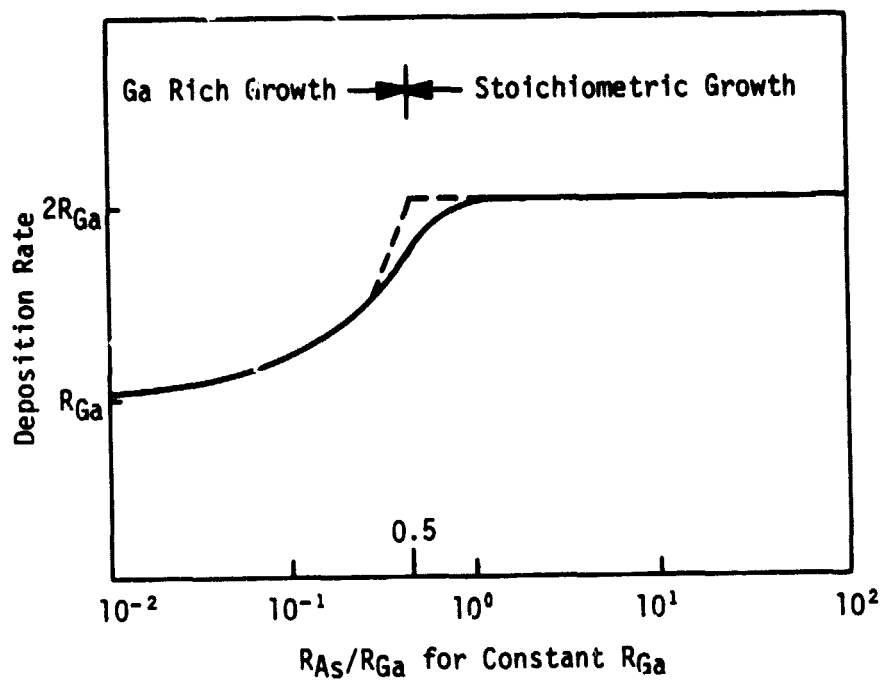


FIGURE 3. DEPOSITION RATE VS. ARRIVAL RATE OF As_2

Present Laboratory Technique:

The apparatus used in the laboratory studies is shown schematically in Figure 4. The growth cell is composed of two graphite segments each having a stainless steel electrode threaded into it (6). The two segments are electrically isolated with boron nitride, and current can flow through the system only when the GaAs substrate is brought in contact with the Ga solution with As in it. Substrates of 1.2 x 1.2 cm area, having thickness between 200 to 300 μm , with (100) crystallographic orientation were employed. A uniform electrical contact between the substrate and graphite was established with a 150- μm -thick Ga layer. The growth cell is placed in a cylindrical furnace with gold reflectors for operational temperature control.

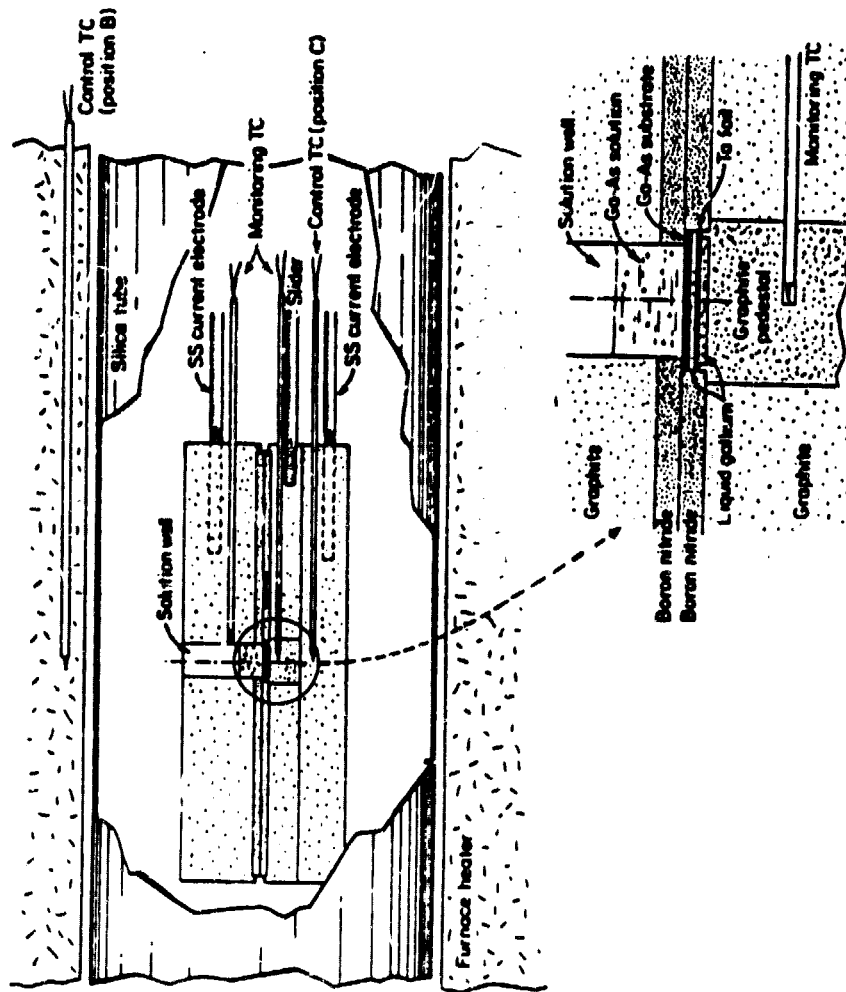
In a typical growth experiment the cell is brought to the desired temperature and the gallium solution is equilibrated using a dummy GaAs substrate for a period ranging from 2 to 5 hr, depending on the quantity of the solution. The real substrate is then brought in contact with the solution, and electrical current is passed through the solution keeping the substrate positive with respect to the solution. The isolation of the real substrate during heat up and equilibration period was necessary to protect the substrate surface from damage.

Experimental Results Important to Space Processing:

The experimental results pertinent to the space experiment facility design and development are presented below. In this context, the dependence of growth rate on current density, process temperature, and solution depth; and the adverse effects of Joule heating and growth current fluctuations are discussed. The data on the dependence of growth rate on current density, etc., are needed for facility sizing and design, whereas the information on the effects of Joule heating and growth current fluctuations are necessary for the facility development so that proper measures can be taken to avoid/minimize these detrimental effects.

Effect of Current Density on Growth Rate - The growth was found to be increasing linearly with current density up to 60 A/cm^2 (7). This is shown in Figure 5 for a temperature of 900 $^{\circ}\text{C}$ and solution depth of 0.7 cm. The growth rate for Si-doped solution was found to be less than undoped solution at higher current density.

Epilayers with the most uniform thickness were obtained at current densities of 50-60 A/cm^2 . At these current densities, the random fluctuations associated with nonuniform current density were counter-balanced by convective flow in solution due to localized Joule heating.



PROCESS TEMPERATURE: 850-975 °C

TEMPERATURE CONTROL: ± 1 °C

PROCESS CURRENT: 10-60 A/cm²

SEED DIMENSION: 1.2 x 1.2 x 0.04 cm

SOLUTION DEPTH: 0.2 - 2.0 cm

CELL RESISTANCE: 0.05 - 0.10 Ω

FIGURE 4. LABORATORY FACILITY

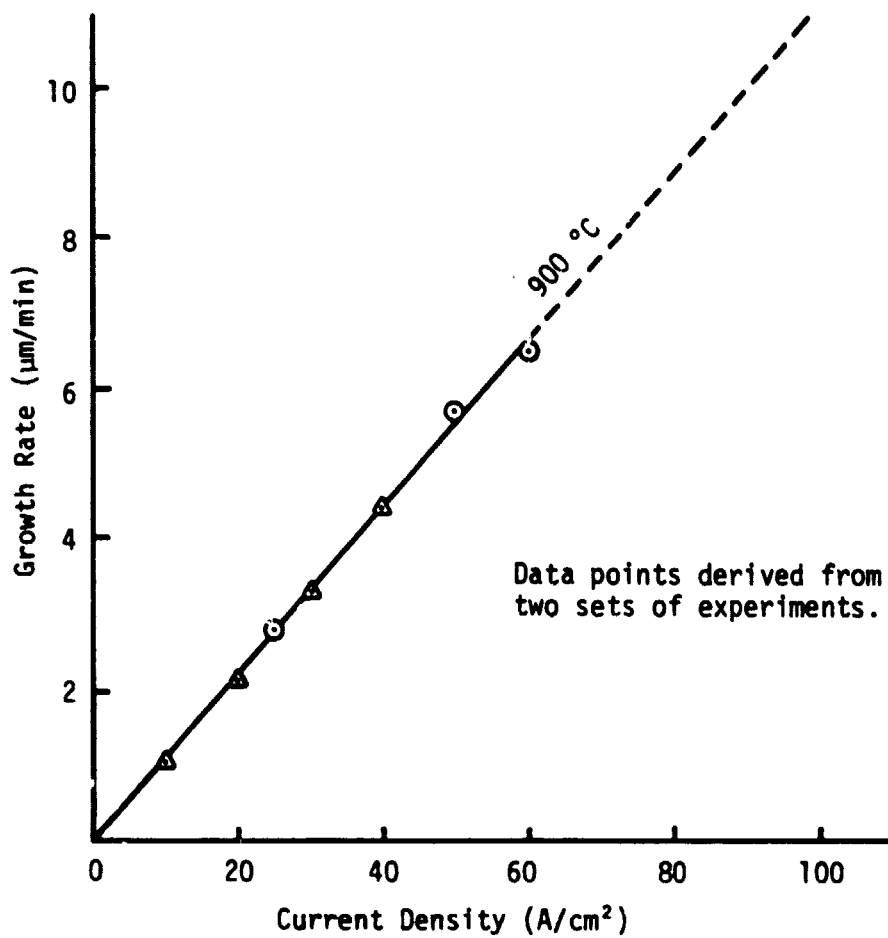


FIGURE 5. EFFECT OF CURRENT DENSITY ON GROWTH RATE

Effect of Temperature on Growth Rate - Figure 6 shows the dependence of the growth rate on temperature under a constant current density of 10 A/cm^2 (7). Below about 825°C it is found that desolution of substrate takes place. At this temperature, growth occurs only upon reversing the current polarity. This phenomenon is also true for the Si-doped solution. The increase in growth rate from $1.6 \text{ }\mu\text{m/min}$ at 950°C to $2.5 \text{ }\mu\text{m/min}$ at 975°C may be an indication of better growth rate at higher temperatures.

The dopant (Si) distribution coefficient increased with increasing temperature and increasing current density

Effect of Joule Heating - Temperature measurements, after thermal equilibrium of the growth cell, were carried out along a horizontal line extending to both sides of the growth cell (6). The results in the absence and presence of 20 amps of current flow are shown in Figure 7.

Joule heating in electroepitaxy establishes a new thermal equilibrium characterized by steeper thermal gradients. In the experimental setup of Reference 6 the thermal gradients, after thermal equilibrium, are found to be a function of the electric power. This is shown in Figure 8. It has been found that Joule heating can play a significant role and introduce defect in the grown single crystal material. Localized Joule heating due to high contact resistance between cell and current electrodes can magnify the problem.

Effect of Solution Depth on Growth Rate - The effect of variation of the solution depth on growth rate is very small at smaller depths. This effect levels out for larger solution depths. This is shown in Figure 9 for a constant current density of 30 A/cm^2 and a temperature of 900°C .

Effect of Growth Current Fluctuation - Nonuniform current density at the growth interface will introduce random fluctuations in the epilayer thickness. Apart from source current fluctuation, the growth current fluctuations can arise from random defects in the electric contact to the substrate or fluctuations in the resistance across the substrate caused by fluctuations in the depth of substrate dissolution by the Ga contact layer.

Gravity Related Crystal Growth Dynamics:

As mentioned earlier, convective flows provide very important sources of enhancing material transfer from the fluid to the growing interface of the crystal. These convective flows can either be natural or forced. There is a multitude of driving mechanisms for natural convection including buoyancy and surface tension. In buoyancy driven convection fluid motions are caused entirely by the action of gravity field on density gradients in the fluid arising from temperature and/or concentration gradients.

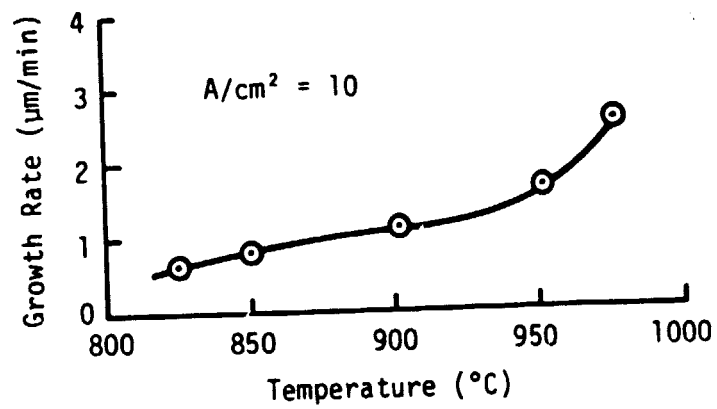


FIGURE 6. EFFECT OF TEMPERATURE ON GROWTH RATE

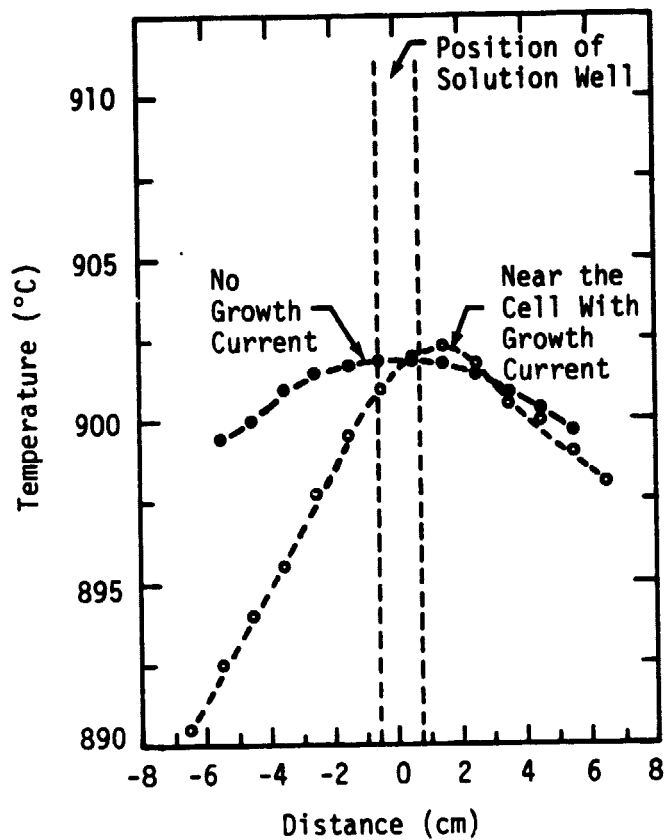


FIGURE 7. HORIZONTAL TEMPERATURE PROFILE
IN GROWTH CELL

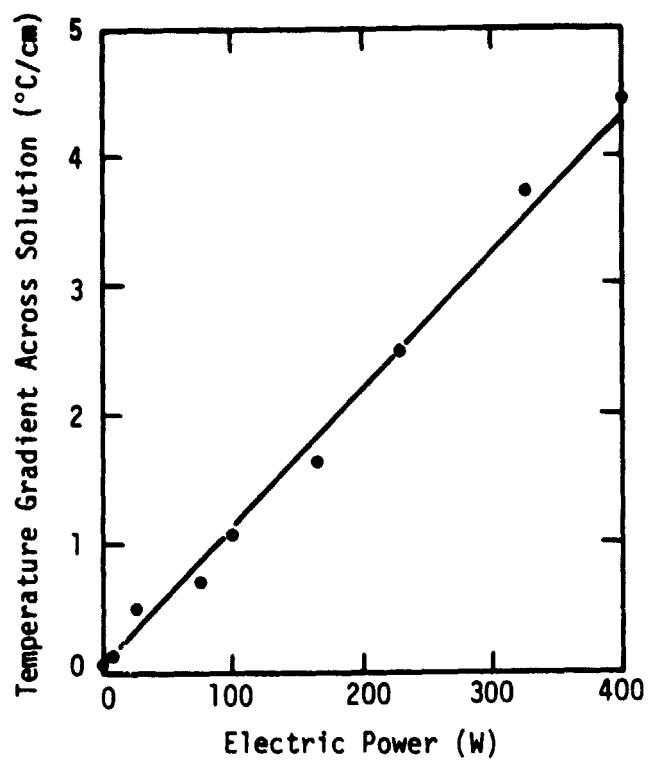


FIGURE 8. TEMPERATURE GRADIENT ACROSS SOLUTION VS. ELECTRIC POWER AT 902°C

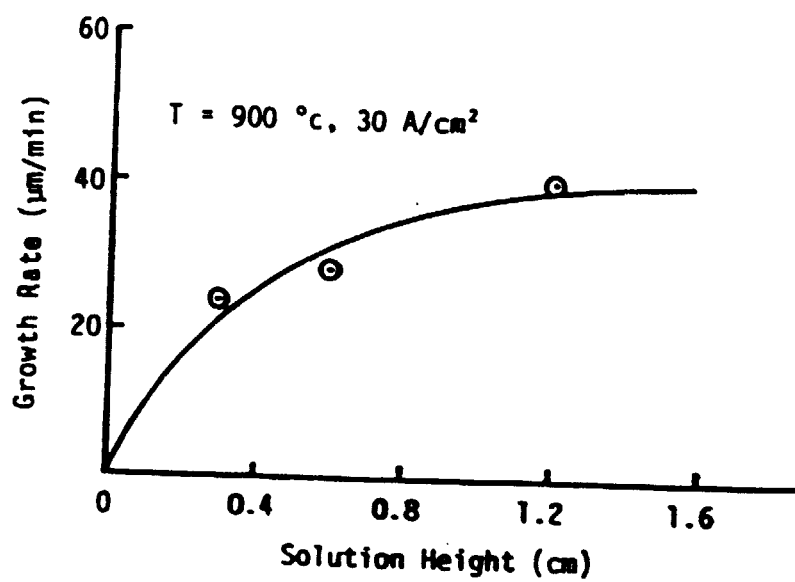


FIGURE 9. EFFECT OF SOLUTION DEPTH ON GROWTH RATE

Thermal Convection - The orientation of the heating and/or cooling surfaces with respect to the gravitational direction is very important in thermal convection flows. The nature of the shear flows generated by both gravity-parallel and -nonparallel heat flows is an important aspect of crystal growth configurations with regard to thermal convection. The thermally driven convective forces can be expressed in a dimensionless form of the Navier-Stokes flow equations. For heat flow parallel to the gravity field, g , the temperature difference ΔT_{\parallel} , is expressed as a Raleigh number

$$N_{Ra} = \frac{g \alpha l_{\parallel}^3 \Delta T_{\parallel}}{\kappa \eta}$$

where α is the thermal expansion coefficient, κ is the thermal diffusivity, η is the kinematic viscosity, and l_{\parallel} is the convective length.

For a gravity-normal temperature difference, ΔT_{\perp} , the driving force is expressed as the dimensionless Grashof number

$$N_{Gr} = \frac{g \alpha l_{\perp}^3 \Delta T_{\perp}}{\eta^2}$$

As the driving force for thermal convection increases the convection cells develop instabilities that result in time-dependent temperature and velocity behavior. Theoretical results on stable and unstable flows for $N_{Ra}/N_{Gr}=1$ are given in the regime diagram depicted in Figure 10 in terms of the Grashof number and the Rayleigh number.

There are many factors which influence the critical Rayleigh or Grashof number at which instability occurs. In general terms, these factors include thermal properties, variations in melt properties with temperature, orientation with respect to gravity field, container geometry, and presence of other body forces.

Chemical Convection - Density gradients due to compositional differences are important for solution growth environment. Solutal convection in isothermal systems is most easily studied by observing the dissolution of solids and measuring the associated mass transport rates. The diffusion boundary layer at a growth interface builds up by segregation processes and, at the point of gravitational instability, releases a blob of solute. The solutal release period can be computed from the solutal Rayleigh number and is predicted to vary with growth rate.

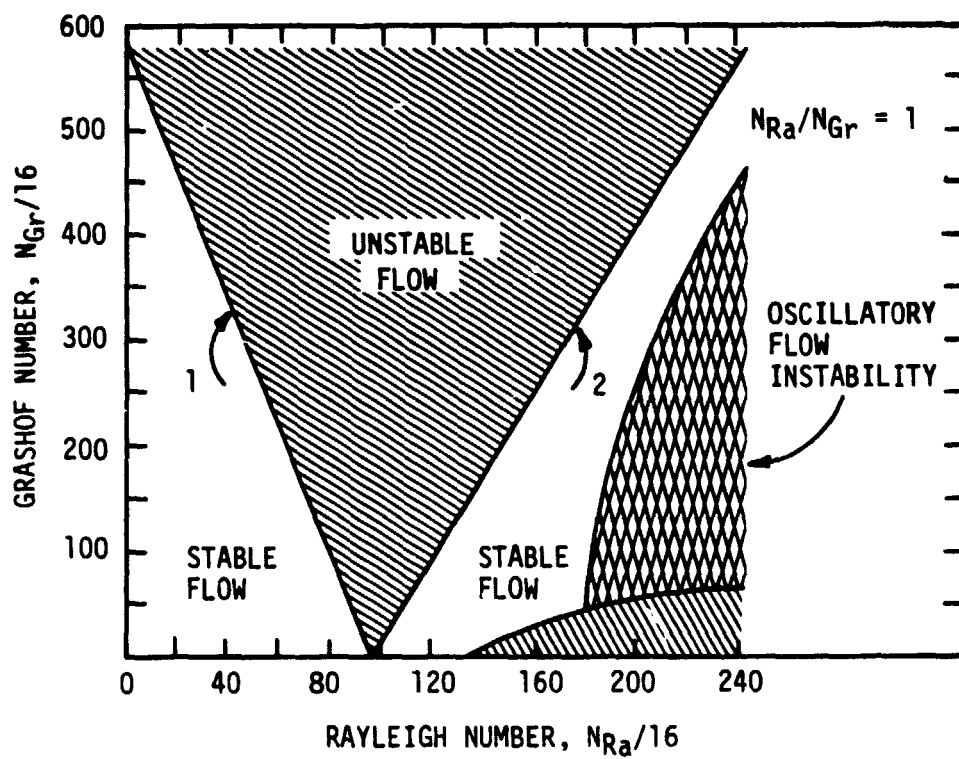


FIGURE 10. STABILITY DIAGRAM FOR CONVECTIVE FLOW

The coexistence of density gradients due to both temperature and composition (thermosolutal convection) is of more interest in crystal growth.

Surface Tension Driven Convection - Surface-tension-driven convection is of particular interest in connection with materials processing efforts in the low-gravity environment of space. On Earth, surface-tension is important only for small-scale configurations, like thin-films, droplets, etc. Surface-tension depends on temperature, composition, and electric field. Horizontal temperature gradient, i.e., ΔT parallel to the free surface can sustain convective flow even in the absence of gravity field. The driving force for the flow is described by a dimensionless quantity called the Marangoni number

$$N_{Ma} = \frac{h^2 \Delta T}{\kappa \eta \rho} - \frac{d\sigma}{dT}$$

where ρ is the fluid density, h is the layer height, and σ is the surface tension. The critical N_{Ma} on Earth for a free surface with no heat flow is $N_{Ma}=80$. There is a tight coupling between Marangoni flow and buoyancy-driven flow such that the thermocapillary convection can be expressed as

$$N_{Ra}/N_{Ra}^C + N_{Ma}/N_{Ma}^C = 1$$

where N_{Ra} and N_{Ma} are the values at marginal stability for the two agencies that reinforce one another. Thus a liquid stable to buoyant forces can still be destabilized by surface tension forces.

References:

- 1) S. G. Epstein and A. Paskin, Phys. Letts. 24A, 309 (1967)
- 2) S. G. Epstein, Advances in Phys. 16, 325 (1967)
- 3) P. P. Kuz'menko, Ye. I. Khar'kov, and V. I. Lozovoy, Phys. Metals and Metallog. 21, 94 (1966)
- 4) J. D. Verhoeven, Trans. Quart. Am. Soc. Metals 55, 866 (1967)
- 5) J. D. Verhoeven, Trans. Met. Soc. AIME 233, 1156 (1965)
- 6) L. Jastrzebski, Y. Imamura, and H. C. Gatos, J. Electrochem. Soc. 125, 1140 (1978)
- 7) L. Jastrzebski and H. C. Gatos, J. Cryst. Growth 42, 309 (1977).